

THE USARRAY TRANSPORTABLE ARRAY AS A PLATFORM FOR WEATHER OBSERVATION AND RESEARCH

BY JONATHAN TYTELL, FRANK VERNON, MICHAEL HEDLIN, CATHERINE DE GROOT HEDLIN, JUAN REYES, BOB BUSBY, KATRIN HAFNER, AND JENNIFER EAKINS

The data, design, and numerous meteorological applications associated with the USArray Transportable Array (TA) seismic network are introduced and discussed.

The USArray Transportable Array (TA) was designed to be a broadband seismic data observation platform to image the subsurface structure of the North American continent. The design of the TA is a nominal Cartesian grid with an interstation spacing of about 70 km. The full TA comprises between 400 and 500 stations deployed simultaneously. The initial deployment of stations started along the West Coast of the United States in 2004, reaching the 400

stations in late 2007. Each station remains in place for approximately two years before being removed from the western edge of the network and then installed on the eastern edge. This “rolling” station deployment strategy gradually migrates the network across the continental United States while recording four continuous seismic data streams at 40, 1, 0.1, and 0.01 samples per second (sps). This has allowed seismologists to construct a composite image of Earth’s interior beneath the surface of the United States revealing the seismic structure in unprecedented detail.

There are numerous benefits to the design and scope of the USArray TA network. First, the data from each station are continuously transmitted and available for monitoring in real time within seconds of collection. The channels at each station are summarized in Table 1. Second, the Cartesian layout of the TA network allows for data to be easily translated into real-world observational, analytical, and research applications. Third, the TA network collects data consistently with a high sample rate at each station. Fourth, all data acquisition systems are phase locked to GPS clocks allowing for synchronous sampling across the whole TA. Fifth, all data are routinely quality controlled by experienced analysts

AFFILIATIONS: TYTELL, VERNON, HEDLIN, DE GROOT HEDLIN, REYES, AND EAKINS—Cecil H. and Ida M. Green Institute of Geophysics and Planetary Physics, Scripps Institution of Oceanography, University of California, San Diego, La Jolla, California; BUSBY AND HAFNER—Incorporated Research Institutions for Seismology, Washington, D.C.

CORRESPONDING AUTHOR: Jonathan Tytell, Scripps Institution of Oceanography, University of California, San Diego, 9500 Gilman Dr., MC-0225, La Jolla, CA 92093-0225
E-mail: jtytell@ucsd.edu

The abstract for this article can be found in this issue, following the table of contents.

DOI:10.1175/BAMS-D-14-00204.1

In final form 4 June 2015
©2016 American Meteorological Society

TABLE 1. Description of the meteorological equipment on board all TA stations, including the names of the channel codes, the parameter sampled with units, and the sampling rates.

Instrument	Channel	Description	Sample rate (sps)
Hyperion Infrasond	BDF_EP	Infrasond (mb)	40
	LDF_EP	Infrasond (mb)	1
Setra 278	BDO_EP	Pressure (mb)	40
	LDO_EP	Pressure (mb)	1
MEMS	LDM_EP	Internal pressure (mb)	1
Vaisala WXT520	LDV_EP	Pressure (mb)	1
	LKO_EP	Temperature (°C)	1
	LIO_EP	Humidity (%)	1
	LRO_EP	Rainfall (mm s ⁻¹)	1
	LRH_EP	Hail (mm s ⁻¹)	1
	LWD_EP	Wind direction (°)	1
	LWS_EP	Wind speed (m s ⁻¹)	1

at the Scripps Institution of Oceanography. All data are delivered to the Incorporated Research Institutions for Seismology (IRIS) Data Management Center (DMC), which provides a free and publicly accessible archive of all USArray TA data. In addition, data from meteorological sensors are processed into 5-min averages and delivered to MesoWest and hence to the National Oceanic and Atmospheric Administration’s (NOAA) Meteorological Automated Data Ingest System (MADIS; Jacques et al. 2015).

Although the USArray TA network is primarily a seismic observatory, its mission has expanded since it was first deployed. It is well known that low-frequency and large-amplitude acoustic signals in the atmosphere, commonly known as infrasond, couple to seismic waves at Earth’s free surface and are readily recorded by seismometers (Kanamori et al. 1991; Langston 2004; de Groot-Hedlin et al. 2008; Arrowsmith et al. 2010; Hedlin et al. 2012a,b). Seismic data from the TA have been utilized to determine source locations of infrasonic signals related to a wide variety of natural and anthropogenic sources at the free surface or in the atmosphere (Hedlin et al. 2010; Walker et al. 2010). The vertical component seismic data were migrated together and a catalog of infrasonic events was constructed to isolate specific “acoustic hotspots” in the western United States within the early USArray footprint (Walker et al. 2011).

It should also be noted that seismic recordings are influenced by daily cyclical fluctuations of air temperatures and wind speeds, effectively imposing a tilting motion onto the ground, and can create a long-period background noise signature on seismic

stations (Sorrells et al. 1971; De Angelis and Bodin 2012). The seismic noise in vertical channels can be reduced at frequencies lower than 2 mHz, however, by subtracting the barometric pressure data from the gravity record at each station (Zürn and Widmer 1995).

The work on atmospheric acoustics mentioned above became the motivation to outfit every TA station installation with one VTI Technologies SCP1000 microelectromechanical systems (MEMS) barometer for monitoring surface barometric pressure at 1 sps, starting in summer 2009. The National Science Foundation’s Major Research Instrumentation-Recovery and Reinvestment project provided additional pressure sensors that were installed at each new station starting in January 2011. These comprise the Setra 278 barometer and the Hyperion infrasond microphone (referred to in previous literature as the “NCPA infrasond microphone”). Both the Setra and the Hyperion sensors are sampled at 40 and 1 sps. By combining all three pressure sensors in this manner, atmospheric pressure changes are recorded across the entire frequency band from DC to 20 Hz (Fig. 1).

As of early 2011, each new TA station was equipped with all three pressure sensors running concurrently, becoming a standard installation feature at all TA stations along with the three-component broadband seismometer (Fig. 2). Every TA station is therefore capable of recording atmospheric phenomena in real time with a minimum sample rate of 1 sps. These features make the TA platform highly suitable for surface pressure monitoring at an availability and detail that the National Weather Service (NWS) does not provide.

As of the time of this paper's publication the TA network has completed its initial planned deployment, with a dataset of surface barometric pressure recordings that covers the eastern half of the contiguous 48 states (Fig. 3a). Station deployment maps and movies can also be accessed online (<http://anf.ucsd.edu/stations.php>).

The TA sensor suite has also facilitated additional weather-related research. TA stations are being utilized for the detection of long-period gravity waves (~6 h) related to severe weather outbreaks (de Groot-Hedlin et al. 2013) and airflow over topography. It is also possible to observe surface pressure fluctuations associated with gust fronts and pressure couplets related to thunderstorm cells of varying severity (Tytell et al. 2011). Furthermore, these surface pressure fluctuations have been identified within the seismic data via direct crustal deformation (Vernon et al. 2011).

In March 2013, 25 of the newly installed TA stations were introduced with a slightly modified configuration that included a Vaisala WXT520 weather station. This added the capability of monitoring several more environmental parameters at 1 sps including humidity, temperature, rainfall, hail, wind speed, and wind direction. The Vaisala equipment at each of the 25 stations was installed at a height of 1.5 m on top of the solar panel mast (see Fig. 2). The configuration might not be optimal for the collection of the wind data for meteorological research, especially since the NWS standard is to monitor wind at 10 m. For thermodynamic comparisons, however, this configuration can be beneficial for meteorological applications since the thermodynamic data are sampled at a station height similar to the NWS and are recorded at a much higher resolution than what the NWS provides (as will be shown in the next section). The footprint for these 25 upgraded stations (Fig. 3b) was chosen to coincide with a large number of surrounding stations from the NWS for the purpose of data validation. In this paper we will refer to this portion of the TA network as the "full meteorological" (full-met) array.

Though the USArray TA network has proven to be extremely useful to the geophysical data community, the goal of this paper is primarily to inform the meteorological community of this dataset and its potential utility for meteorological studies. We will address applications for observational meteorology as well as potential research endeavors that can be accomplished with both the archived TA data and with data that are continuously being supplied via the instruments still deployed in the field. We will also demonstrate the feasibility of the TA network's configuration for future similar cross-disciplinary networks.

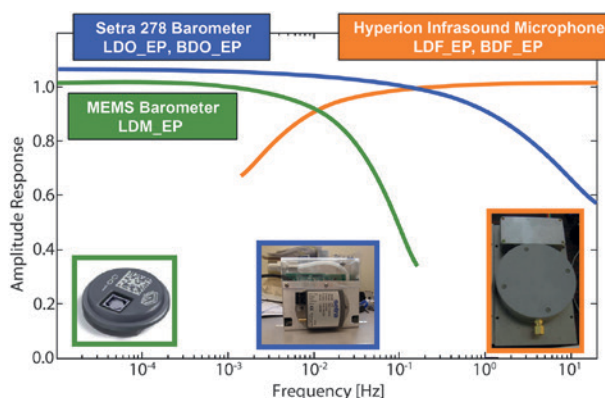


FIG. 1. Graph of relative amplitude response of the three pressure instruments at each TA station [MEMS barometer (green), Setra 278 barometer (blue), and Hyperion infrasound microphone (orange)] vs frequency. The three instruments collectively sense the entire frequency range between DC and the Nyquist frequency. Pictures of each instrument are shown, and the channel codes for each instrument are also indicated. Channel codes beginning with "B" acquire data at 40 sps, whereas those starting with "L" acquire data at 1 sps.

DATA QUALITY VALIDATION. To introduce the quality of the pressure data recorded by the TA, we must first discuss how pressure is sampled at each station. Issues regarding the potential effects of dynamic pressure on recorded pressure data (Bedard and Sanders 1978) led researchers to utilize specially fabricated pressure inlet systems in order to reduce this effect (Nishiyama and Bedard 1991; Lee et al. 2004). For the TA platform a similar approach was taken. A 3/4-in.-diameter hose (1 in. = 2.54 cm) connects from the internal pressure-monitoring equipment through the side of the vault bulkhead and into a bag of pumice rock several feet away from the vault. The tube is turned to face downward. At the end of the pressure inlet tube is a specially manufactured diffuser: a 4-in.-diameter PVC cap encasing a thick ring of rigid plastic that twists onto the end of the pressure inlet hose. Along the sides of the diffuser approximately one dozen roughly 1/8-in.-diameter holes are drilled concentrically through to the center cavity and spaced about 1 in. apart, with one more hole drilled into the top end of the PVC cap. The diffuser, pumice, and tube orientation help to reduce the dynamic pressure effects of wind onto the pressure inlet tube and prevent water and dirt from getting into the tube.

Over the course of its deployment, 20 of the TA stations were installed relatively close (<5 km) to NWS quality controlled stations that provide local

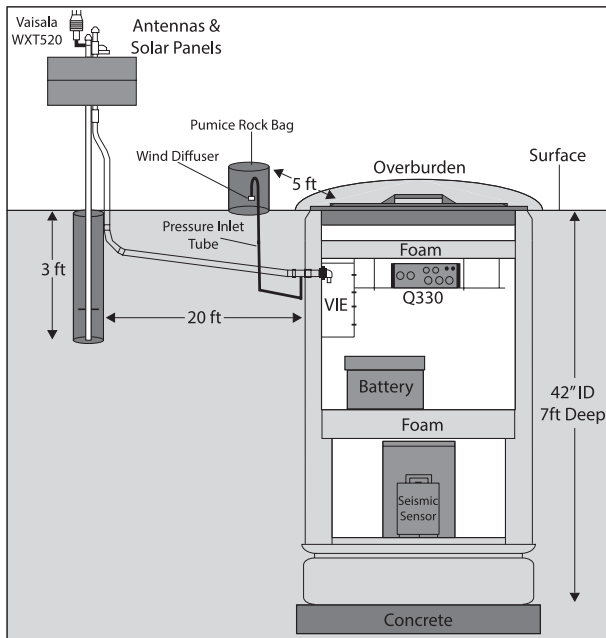


FIG. 2. Standard configuration of each USArray TA station. Vault enclosures reach about 7 ft (2.13 m) below the surface with the seismometer housed in the base section on top of a bed of concrete. Below the lid of each vault is the Q330 datalogger, and next to that is the vault interface enclosure (VIE), which holds several pieces of equipment including the data storage devices (balers), MEMS barometer, Setra 278 barometer, and Hyperion infrasound instruments. Backup power is provided by a battery in the midsection of the vault. A pressure inlet port containing a 3/4-in.-diameter hose connects from the three pressure sensors within the VIE, through the side bulkhead of the vault, and into an external bag of pumice rock several feet away from each vault. At the end of the pressure inlet tube is a specially designed diffuser to help reduce the dynamic pressure effects of wind into the bag of pumice rock. Several feet away from each vault are the solar panels and telemetry. The location of the Vaisala WXT520 weather station is indicated for those stations that are part of the full-met array.

climatological data. This gives us an opportunity to compare data from both. One example is TA station U58A, which is the only station of the 20 that is also part of the full-met portion of the TA network. This station is situated approximately 4.2 km away from the NWS station near Oxford, North Carolina (KHNZ). Since the two stations are at roughly the same altitude (157 and 169 m, respectively) and surrounded by similar terrain, they can provide a reference point for assessing the quality of TA stations with a Vaisala WXT520 installed. By examining data from both stations during a gust-front passage (Fig. 4), we can immediately see the benefit of the

higher sample rate of a TA station when compared with an NWS station. Throughout Fig. 4, we see only three data observations from KHNZ over the entire hour versus the 1- and 40-sps observations at U58A. Figure 4a displays the 40-sps Setra barometric pressure data from U58A as compared with data from NWS station KHNZ, while Fig. 4b shows the relative humidity, and Fig. 4c depicts the temperature and dewpoint temperature [calculated manually for TA; Wallace and Hobbs (1977)] at both stations. Basic features associated with a gust front passage at around 1600 UTC are also shown throughout Fig. 4 including a pressure jump (Fig. 4a) followed by an increase in humidity (Fig. 4b) and a temperature drop (Fig. 4c). Patterns from the U58A data agree with those observed from KHNZ, although it is clear that KHNZ's low sampling resolution does not capture enough detail to accurately reflect the timing or magnitudes of these localized changes.

POTENTIAL METEOROLOGICAL CONTRIBUTIONS. The configuration of a standard TA installation presented in Fig. 2 allows for two separate branches of meteorological observation and research: 1) study of mesoscale and synoptic-scale weather phenomena using several stations from the array and 2) real-time monitoring of localized weather phenomenon.

Mesoscale to synoptic scale. There are numerous mesoscale- and synoptic-scale-based applications that make use of the Cartesian-style footprint of the TA network. As mentioned previously, one ongoing and active area of research is in the location and cataloging of infrasound sources (Walker et al. 2011). Our group has also been building a catalog of gust front, mesohigh, and wake-low events from severe thunderstorms since their surface pressure features are easily identified when they pass directly over TA stations. Careful analysis of these surface pressure features may permit the design of a real-time detection system of storm events and may also augment nowcast decision-support capabilities. Furthermore, the full-met portion of the TA network displays how a similarly constructed array can provide additional insight into the severity of weather systems with real-time analysis of temperature and humidity changes.

Current research involves the use of the TA station footprint to detect gravity waves with periods greater than 40 min. In a recent study (de Groot-Hedlin et al. 2013), TA data recorded during the April and May 2011 tornado season were examined to identify where gravity waves were being generated and

to track their subsequent travel across the TA. The entire TA was subdivided into a large number of non-overlapping three-station subarrays of roughly similar sizes and shapes using a Delaunay triangulation method. Waveform cross correlations were computed over sliding time windows at each of these “triads” to detect coherent arrivals; if signals were coherent over a given time window, the phase velocity and propagation direction were estimated. The results were examined over the ensemble of triads to find regions in which neighboring groups of stations provide consistent detections for any given time window, thus providing a discretized approximation of a continuous gravity wave moving across the array. Figure 5 shows a map of low-frequency pressure data and associated gravity wave detections for a 10-h time window centered at 0300 UTC 27 April 2011. A map of brightness temperature perturbations, as measured by the Atmospheric Infrared Sounder (AIRS) satellite, indicates the presence of a large-scale gravity wave in the altitude range from 20 to 65 km over the eastern half of the United States for this time period (L. Hoffmann, Jülich Supercomputing Centre, 2014, personal communication). The coincidence of our low-frequency pressure signals across the TA with stratospheric gravity waves suggests that TA data may be useful for studies of atmospheric gravity waves or other large-scale atmospheric phenomena.

The TA network has also been used to analyze mesoscale and synoptic features, such as those related to squall lines and tropical storms, purely through

use of the seismic observations. This has created new applications of larger-scale weather data. In 2012, as Hurricane Sandy was moving north along the East Coast, seismic vibrations from waves crashing along the shoreline were detected hundreds of kilometers inland (Sufri et al. 2013).

More recently, TA seismic data were used to compare with the NWS Automated Surface Observing System (ASOS) network within central Illinois in order

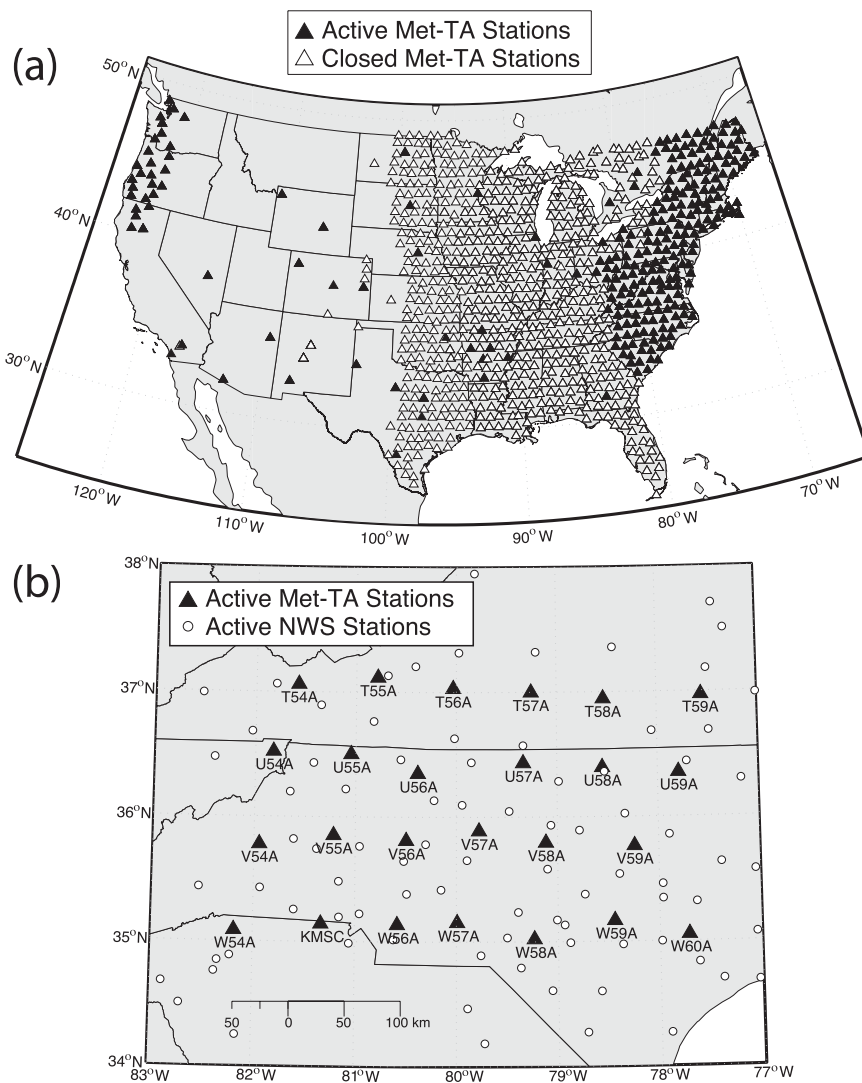


FIG. 3. (a) Cumulative map of the USArray TA meteorological deployment as of the end of Jan 2014. Black triangles are actively deployed TA stations, while white triangles were previous TA sites that have since been decommissioned. (b) Map of the 25-station full-met USArray TA footprint (black triangles), located mostly throughout NC and southern VA. Two of the TA stations are in SC. White circles refer to NWS stations that provide quality controlled local climatological data. The area for this full-met footprint was chosen to coincide with the higher volume of NWS stations within this region rather than in other areas of the contiguous United States, where NWS station coverage is usually more sparse.

Data Quality Comparison NWS Station KHNZ vs. TA Station U58A on 2/21/14

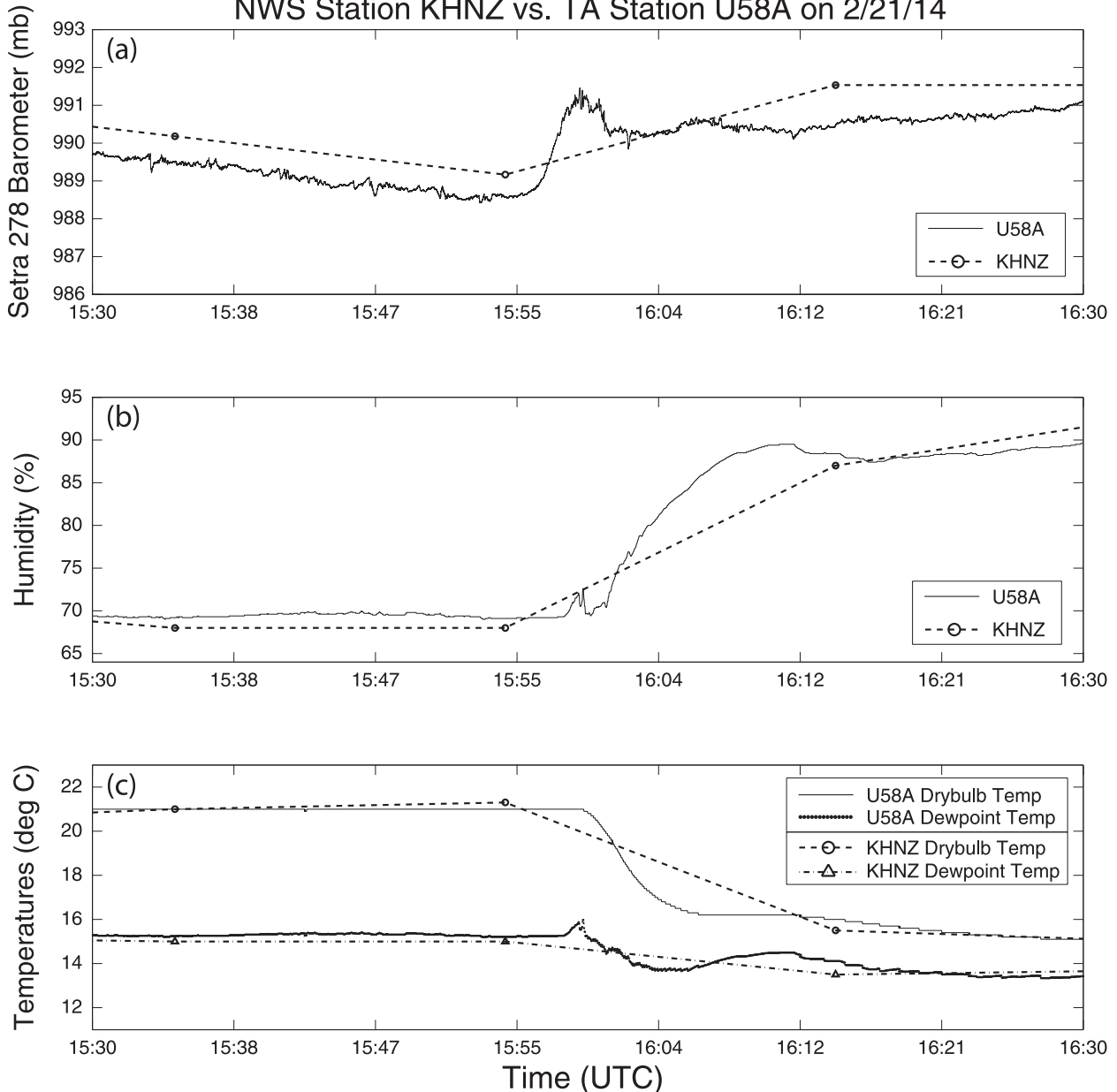


FIG. 4. (a) The 40-sps Setra 278 barometer data from U58A (solid line) are plotted against data from NWS station KHNZ (dashed line, circles) during a small gust-front passage on 21 Feb 2014. Several pressure features are apparent within the MEMS data that are missed by the NWS data, including a pressure jump of about 2 mb around 1600 UTC. (b) The Vaisala I-sps relative humidity data from U58A (solid line) are plotted against the same parameter from KHNZ (dashed line, circles) where the RH is shown to increase by about 20% within 10 min. (c) Vaisala I-sps temperature values from U58A (solid line) are plotted against the same value from KHNZ (dashed line, circles), showing a temperature drop of about 5°C within 5 min. Meanwhile, using the Clausius–Clapeyron equation and the latent heat of vaporization, we can calculate the dewpoint temperature at U58A (dotted line) from temperature and relative humidity values and plot them against the same parameter from KHNZ (dashed line, triangles) to show how saturated the air becomes after the gust front’s passage.

to characterize wind speed observations from a large number of high-wind events (Pryor et al. 2014). In this study it was shown that well-defined spectral signatures

within the TA seismic data appeared to correspond with wind-gust events. Furthermore, the maxima from these signatures had the tendency to scale with the intensity

of the observed wind gusts. Ultimately, Pryor et al. find that the TA's 40-sps seismic data were better suited for observing surface pressure variability on a subsynoptic scale than the ASOS network even despite the density of the ASOS coverage. This feature may allow for the TA network to be used for spatially mapping and characterizing gust-front events, though additional research is necessary. In order for NWS stations, including ASOS, to match the TA for this potential capability, they would either have to record much-higher-resolution data than the standard one to three samples per hour or their station distribution density would have to be much greater.

Additionally, when examining the data from the TA network on larger scales, it is possible to validate and tune weather prediction models. This certainly applies to pressure models as every TA station has the capability of observing pressure changes not only through the barometric pressure and infrasound installation suite, but also with seismic response observations. Gravity wave observations may provide validation for upper-atmospheric models.

Finally, because of the spacing between individual TA stations, the TA network can be used for visualizing the synoptic-scale pressure field and can contribute to the pressure readings for real-time surface analysis maps.

Local scale to mesoscale. In regard to localized weather phenomena there are numerous avenues for observation and research. The ability to utilize data at 1 and 40 sps in real time marks a rare meteorological opportunity for observing high-frequency atmospheric events from local origins.

GUST FRONTS. Downbursts and gust fronts from thunderstorms are aspects of severe weather that are capable of posing significant risks to life and property because of their high-velocity winds. Fujita and Byers

conducted a detailed case study of an airliner crash at John F. Kennedy International Airport in New York in 1975 that resulted from a strong downburst (Fujita and Byers 1977). This tragic event led to further research on downbursts and subsequent gust fronts for several decades (Bedard et al. 1977; Houze 1993; Klimowski et al. 2003; Atkins et al. 2005).

One method for identifying gust-front passage is with Doppler radar products from the Next Generation Weather Radar (NEXRAD) program (Klingbe et al. 1987). Using the reflectivity scans at the lowest angle (5°), it is possible to view arc clouds that form above the rolling head of most gust fronts. With this method it is possible to track the speed and movement of a gust front; however, not all gust fronts produce arc clouds and the 5° scan angle can actually overshoot these clouds with greater distances. Furthermore, these Doppler scans cannot provide feedback for changes in wind speed and pressure directly at the surface.

The nature of the TA network does not allow for direct upper-air investigation like a Doppler scan, but we can achieve very-high-detail observations at the

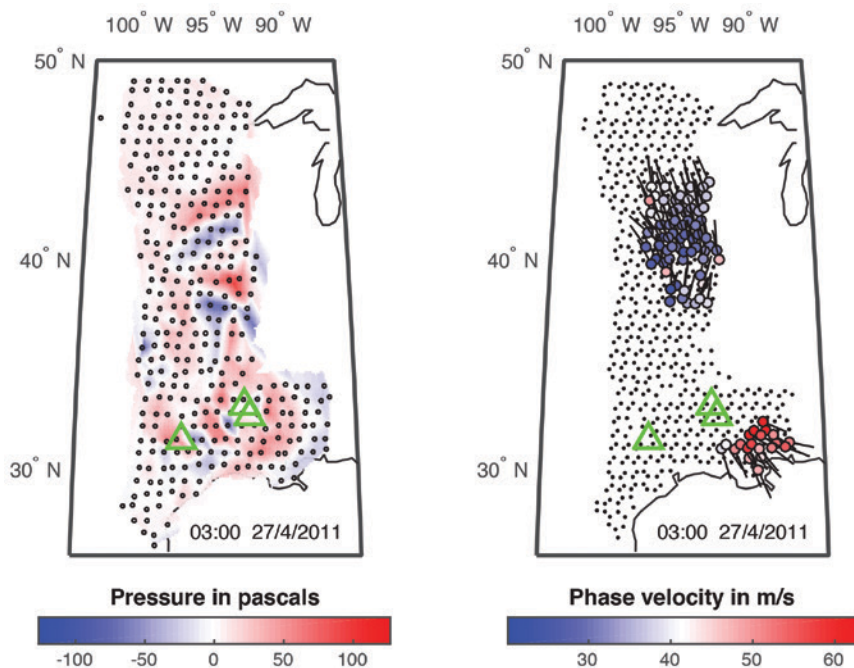


FIG. 5. (left) Snapshot of the TA pressure data, bandpassed from $T = 2$ to 6 h and spatially interpolated between stations, at 0300 UTC 27 Apr 2011. Circles mark station locations. The large green triangles denote tornado locations from the NWS that occurred within 15 min of the time stamp. (right) Gravity wave velocities and directions of motion are shown. Travel directions and azimuths were computed for each group of three neighboring stations. The dots indicate the centers of triads that did not register a gravity wave. Circles mark the centers of triads where gravity waves were detected, color-coded by the horizontal wave speed. The black line attached to each circle indicates the direction of wave propagation.

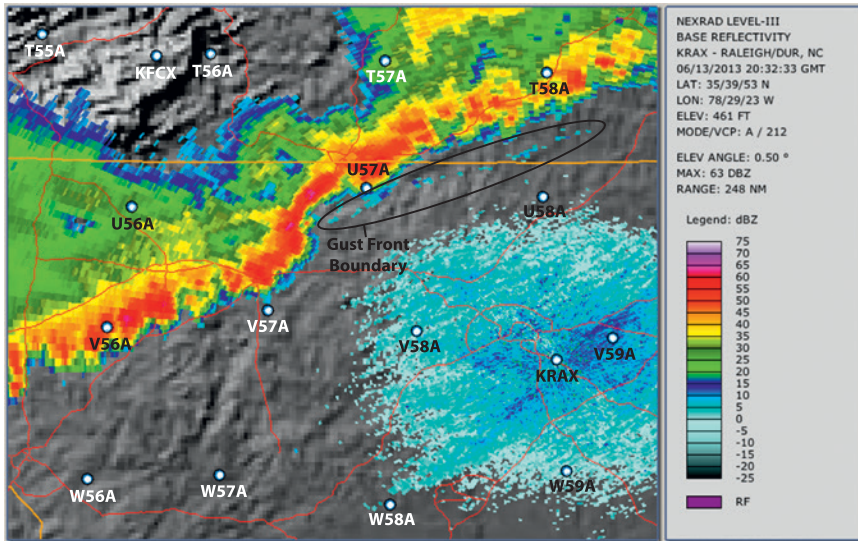


FIG. 6a. KRXZ image depicting a squall line following the 13 Jun 2013 derecho through the full-met array. For this image, the base reflectivity product with a scanning angle of 0.5° is used in order to isolate an arc cloud associated with the gust front that was generated from this squall line. An oval has been overlaid on the image indicating the general location of the arc cloud. The track of this gust front with time at TA stations U57A, V57A, and W57A is also shown. The image was developed using the NOAA Weather and Climate Toolkit.

surface. This makes the platform suitable for gust-front monitoring. Pressure jumps and even overturning pressure within the gust-front head can often be seen within the TA data, including the seismic data.

To illustrate this capability, we show TA recordings of pressure changes from a gust front that was generated from a squall line following the derecho on 13 June 2013. Figure 6a depicts a Weather Surveillance Radar-1988 Doppler (WSR-88D) image from Raleigh, North Carolina (KRXZ), with surrounding TA stations and a gust front indicated [via the NOAA Weather and Climate Toolkit; Ansari (2014)]. The magnitude of this gust front can be seen at station U57A (Fig. 6b), where a pressure jump of about 2.5 hPa within approximately 4 min marks the arrival of the gust front head at 2024 UTC. Pressure fluctuations at the surface can also be seen in seismic data. Thus, we have included the eastern-oriented seismic channels in both raw and filtered formats. The filtered channel isolates signatures between 0 and 0.1 Hz and helps to identify these seismic perturbations.

As the gust front spreads away from its origin, it is expected to weaken in magnitude, and Fig. 6c does show a slightly weaker gust front arrival at V58A, located approximately 74 km SSE of U57A. The gust front arrival here is at 2120 UTC, roughly 1 h after it crossed U57A, with a pressure jump of approximately 2 hPa in 4 min. This implies an average travel speed of

about 74 km h^{-1} (20.6 m s^{-1}) if we were assuming laminar flow across the terrain. We can also see an additional increase in pressure by about 1 mb behind the gust front arrival at V58A, possibly because of the overturning air within the gust front head pressing against the surface.

Figure 6d reveals the weakening of the gust front with time and distance. By the time the gust front reaches W58A around 2230 UTC, it has traveled about 160 km directly south from U57A, or about 86 km SSW from V58A. The pressure jump is more of a gradual ramp-up of 1.5 mb over 10 min with little seismic perturbation. If we were to assume laminar flow again during this second half of the journey, it

would imply that the gust front still traveled at around 74 km h^{-1} (20.6 m s^{-1}). While the magnitude of the pressure jump has diminished, the travel speed in the southern direction has not.

The applications for historic gust-front investigation are apparent, but the real-time applications for potential gust-front tracking should not be overlooked. Combining the pressure-jump arrival times and magnitudes from several stations may allow us to infer the direction and speed in which a gust front will travel. Further combination with Doppler radar scans would be even more beneficial. Additional observations from the TA's full-met stations, including temperature, humidity, and wind speed and direction changes, can be highly useful for nowcasting gust-front movement from a smaller scale.

SEISMIC SIGNATURES POTENTIALLY RELATED TO TORNADES. A tornado releases energy into the ground in the form of heat and high-frequency vibrations (Tatom 1993; Tatom et al. 1995; Tatom and Vitton 2001). One of the challenges with severe weather nowcasts is determining whether a vortex is actually on the ground. Doppler observations of hook echoes and velocity couplets are commonly used for tornado vortex identification; however, that does not necessarily translate to the vortex being on the ground. Perhaps the most common method for identifying this is via eyewitness weather reporting from spot observers.

TA Station/Channel Comparison on 6/13/13

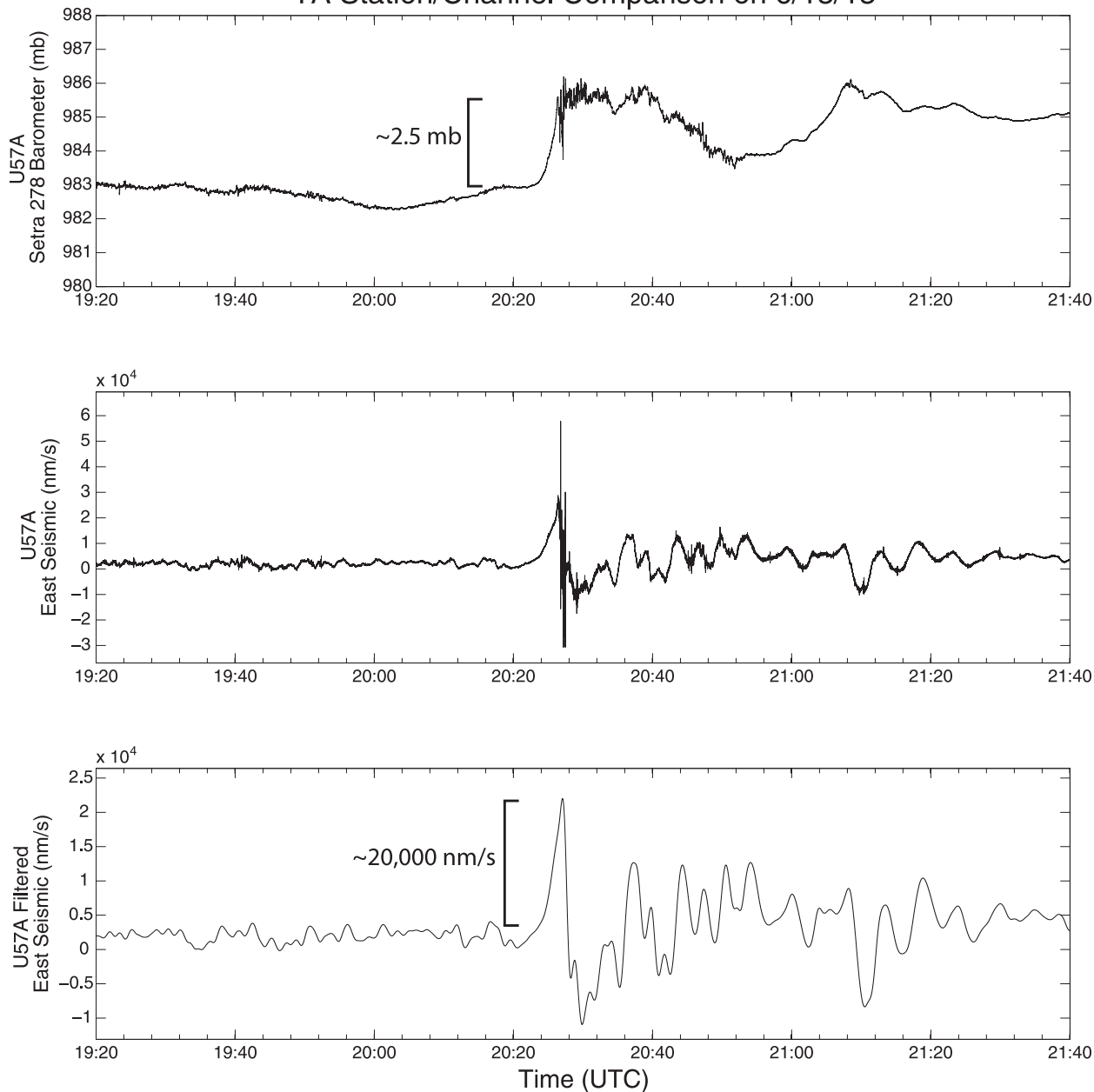


FIG. 6b. A comparison of (top) the 40-sps Setra 278 barometric pressure data at TA station U57A with (middle) the raw east seismic component. (bottom) As in (middle), but with a 0–0.1 Butterworth bandpass filter applied. The 2.5-mb pressure jump depicted in (top) around 2028 UTC correlates well in time with crustal perturbation. There is further crustal perturbation coinciding with the rise in pressure around 2110 UTC.

Periodically, some of the stations within the TA network (<12) have experienced close pass-bys from tornadoes within 10 km. Many of these coincided with the 2011 tornado season, where historic outbreaks occurred during April and May across large portions of the southern and central regions of the United States (Doswell et al. 2012). On 27 April 2011, there was a tornado rated as category 3 on the enhanced Fujita scale (EF3) that crossed through Chickasaw and

Monroe Counties in northeastern Mississippi (www.srh.noaa.gov/meg/?n=apr2011toroutbreaknewwren). Based on start- and endpoint tornado track data provided by the Memphis, Tennessee, National Weather Service Forecast Office, the tornado apparently passed well within a few kilometers to the northwest of TA station Y46A. The seismic data during this pass-by revealed a clear tilt of the crust (Fig. 7), potentially because of the tornado being located near Y46A. If a

TA Station/Channel Comparison on 6/13/13

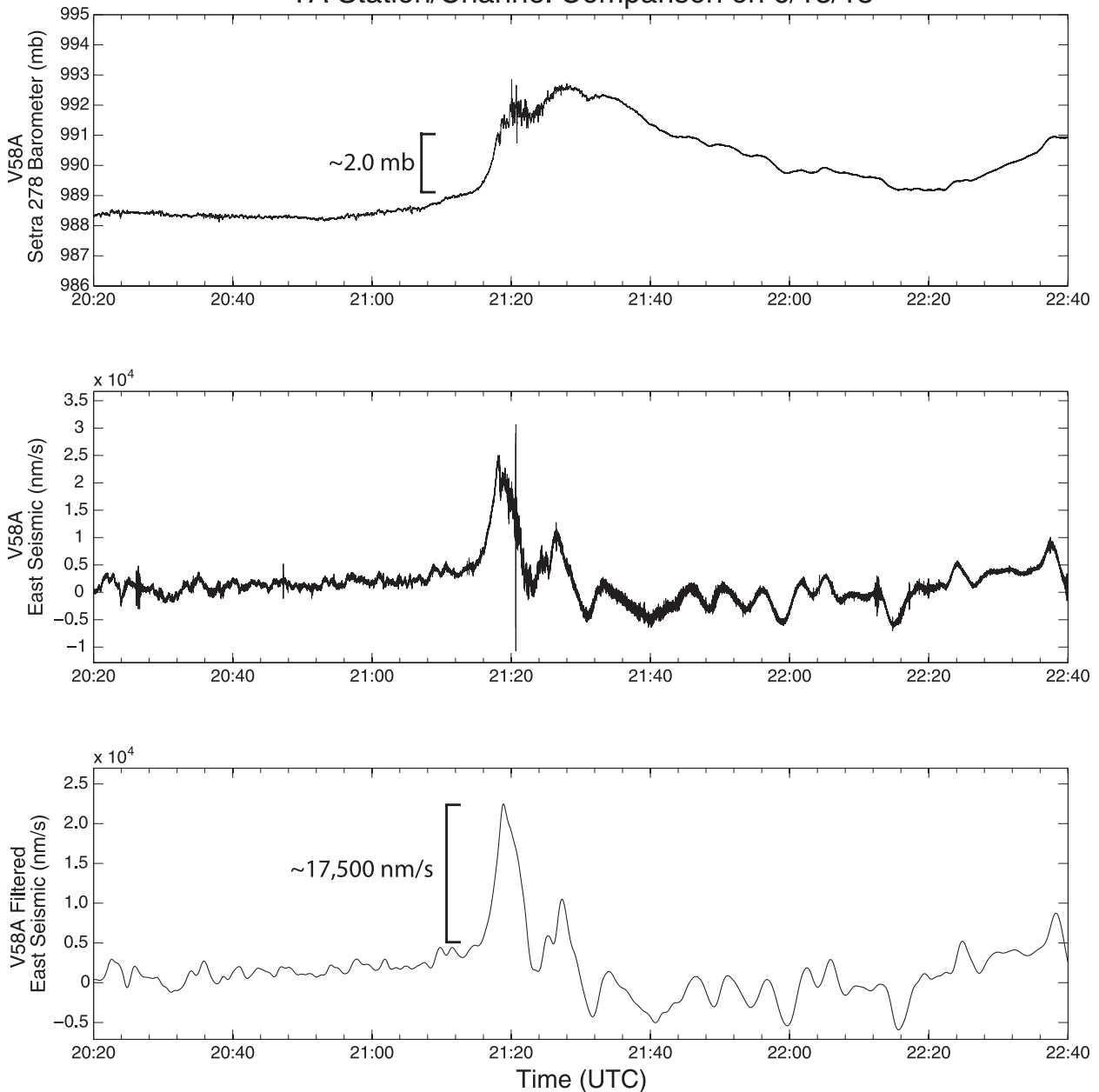


FIG. 6c. As in Fig. 6b, but for TA station V58A. In this case, the pressure jump has a slightly smaller magnitude (~2.0 mb) around 2120 UTC in 4 min with a gradual increase in pressure afterward likely due to the overturning circulation in the gust-front head. The magnitude of the coincident crustal perturbation is slightly smaller than at U57A as well.

real-time seismic network can supplement Doppler observations and help to determine if a tornado is present, then this information can be invaluable for assisting with the production of nowcasts and early warning detections.

Additionally, the TA is potentially capable of isolating a unique vibration signature of tornadoes when they are close. It may require higher-frequency data, but conceivably a unique acoustic signature from these tornadic vibrations can be used for constructing

warning alarms to alert people to head to their basements (Tatom 1993). This avenue of research is currently on going. We do not currently have an algorithm constructed to detect tornadoes within the TA data, but we are working on a database of tornado events that includes their distances from individual TA stations for as many events as possible.

RAINFALL TOTALS. One of the data channels available to each Vaisala WXT520 weather station monitors

TA Station/Channel Comparison on 6/13/13

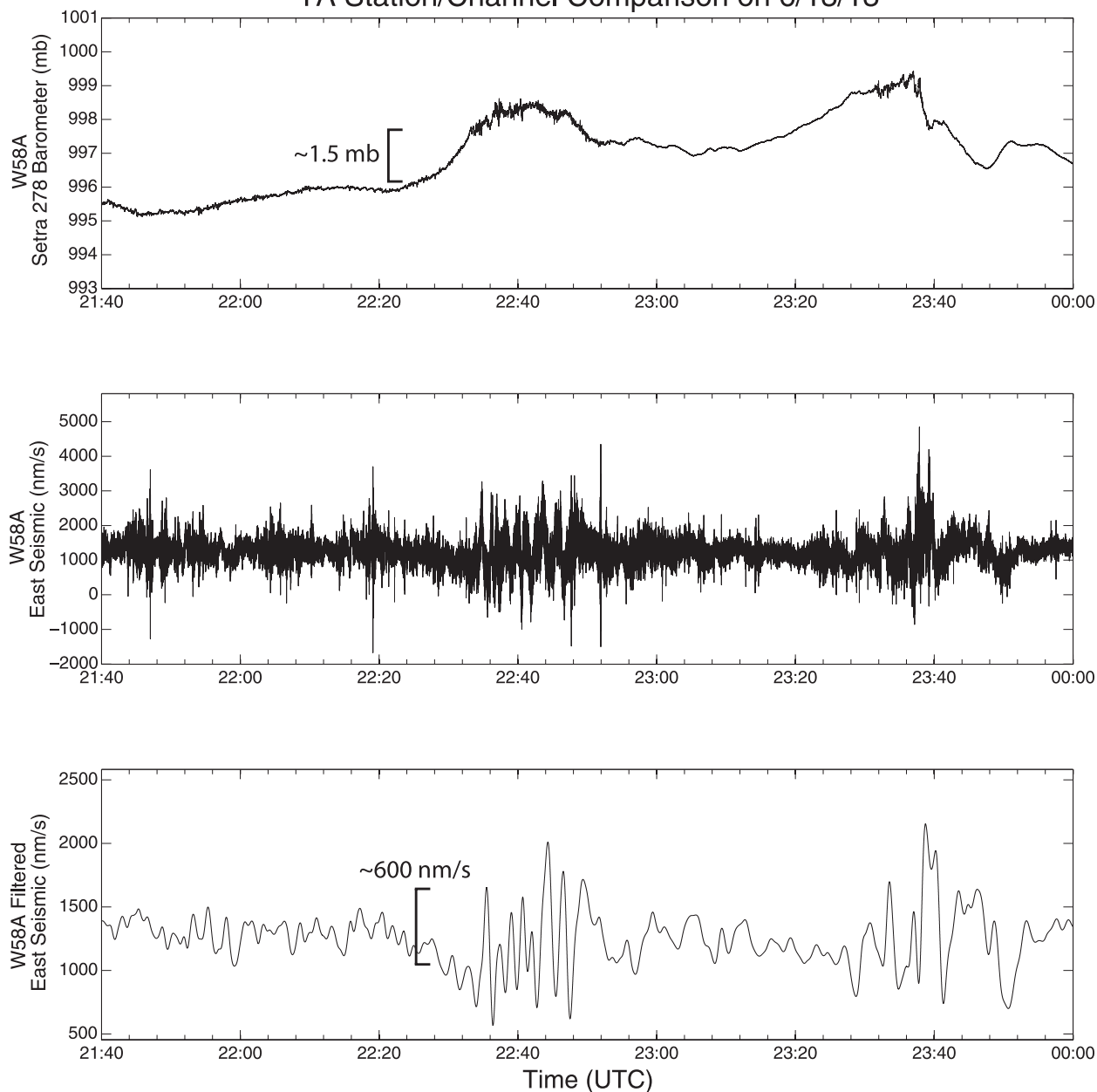


FIG. 6d. As in Fig. 6b, but for TA station W58A. In this example, the pressure jump occurs around 2230 UTC and is more of a gradual ramp-up overall of about 1.5 mb. There is small but measurable crustal perturbation coincident with this arrival as well. An additional pressure drop around 2336 UTC can be seen with the matching crustal perturbation at about the same time.

rainfall, which means each full-met station can serve as an individual rain gauge. By default, these rainfall channels are calibrated for reporting real-time rainfall rates on a per-second basis, which may not necessarily be the most useful data point since the measurement standard is to report a rainfall total over a longer period of time. Converting these rainfall rates into rainfall totals is a simple exercise, though, and can be done for any specified period of

time. The TA's rainfall observations can then be used to compare with other local weather monitoring data and even validate precipitation totals.

Two ways that the NWS acquires its precipitation measurements are from 1-h storm totals at individual ASOS stations or extrapolated from WSR-88D products (Fulton et al. 1998; Istok et al. 2009). Using the latter, it is possible to determine the estimated rainfall total at each of the TA's full-met

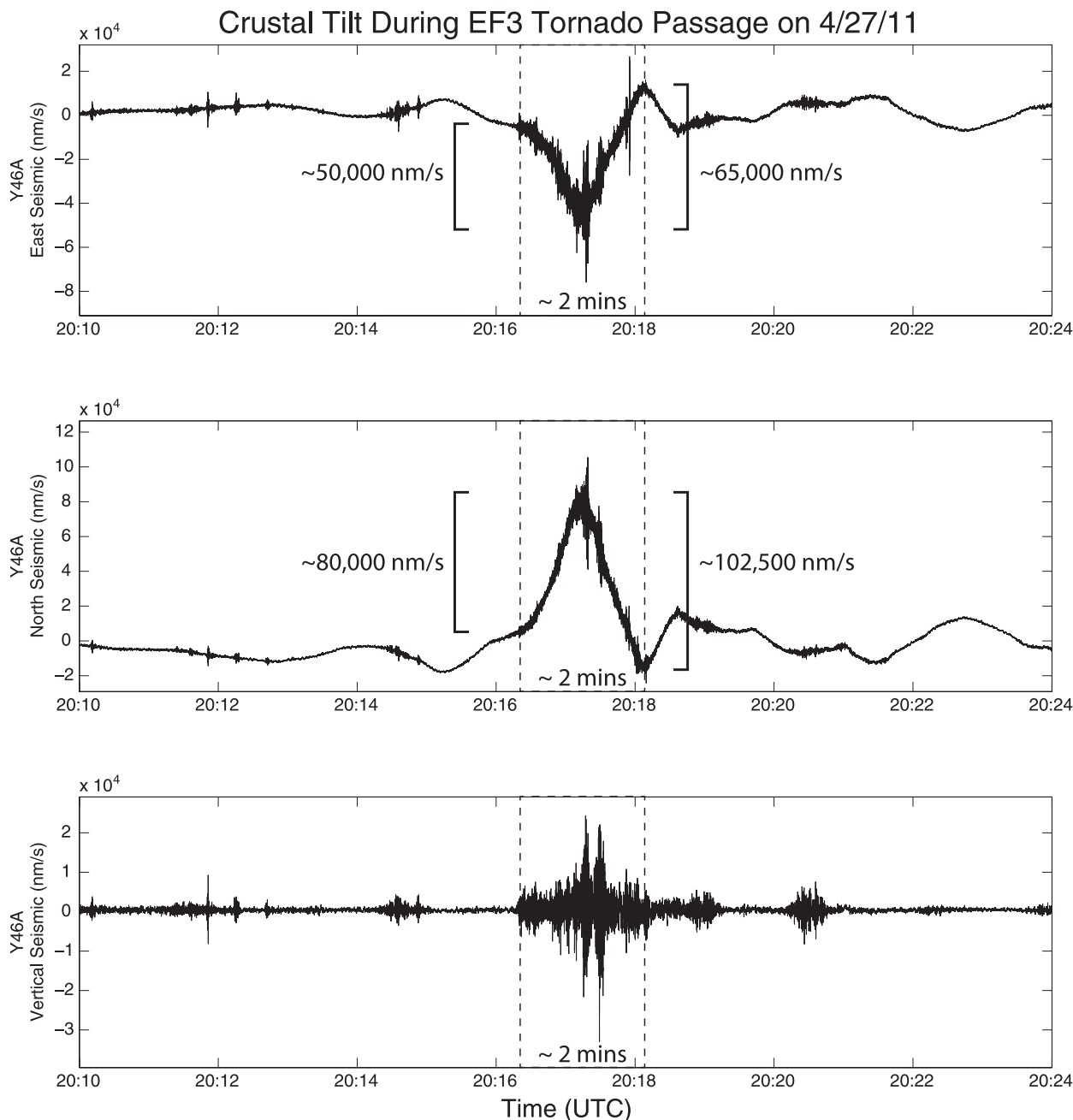


Fig. 7. Seismometer readings from station Y46A during the potential pass-by of an EF3 tornado on 27 Apr 2011 in northeastern MS. (top) The east–west-oriented seismic channel, showing a tilt of the crust in the westward direction. (middle) The north–south-oriented seismic channel showing a similar tilt toward the north. Both tilts are shown to rebound by the end of this 2-min time slice. (bottom) The vertically oriented seismic channel displays a packet of high-frequency vibrations of the crust above and below ground level. The overall tilt is to the northwest, in the direction of the nearby tornado. This suggests that the funnel was on the ground at the time of the pass-by.

stations and compare to actual rainfall observations via the Vaisala WXT520. There are four WSR-88D stations around the footprint of the full-met array: Blacksburg, Virginia (KFCX); Wakefield, Virginia (KAKQ); KRAX; and Greer, South Carolina (KGSP). For this analysis we are using the NEXRAD level III

Digital Storm Total Precipitation product (DSP) from these four Doppler stations during the previously presented squall-line passage on 13 June 2013. Table 2 summarizes the rainfall observations and differences between the two platforms as grouped by the full-met stations' nearest Doppler station. Figure 8a displays

TABLE 2. To assist with the rainfall analysis during the squall line on 13 Jun 2013, we used data from the NEXRAD level III DSP product (as observed via the NOAA Weather and Climate Toolkit). Shown are the rainfall amounts as observed by the WSR-88D vs those observed by the TA stations in the full-met footprint. The Doppler observations were obtained simply by zooming in to each lat–lon of the corresponding TA station and identifying the value of the data layer. The calculated TA totals were obtained via a script that computed each total based on the DSP time-frame window specified in in the second column. The full-met TA stations were grouped according to their nearest Doppler stations.

TA station	WCT DSP time frame (UTC) ^a	Distance from nearest Doppler (km) ^a	WCT DSP total rainfall (in.) ^a	Vaisala TA total rainfall (in.)	Absolute difference from DSP obs (in.)	Relative difference from DSP obs (%)
T54A	0223–2003	116.0	0.3200	0.3842	0.0642	20.1
T55A	0223–2003	46.5	0.5400	0.2561	–0.2839	52.6
T56A	0223–2103	21.6	0.1000	0.0589	–0.0411	41. ^b
T57A	0223–2103	90.9	0.5600	0.5552	–0.0048	0.9
T58A	1210–2201	136.0	0.2400	0.3633	0.1233	51.4
T59A	1210–0000 ^c	48.7	0.3100	0.3074	–0.0026	0.8
U54A	0223–2103	149.0	0.2600	0.4657	0.2057	79.1
U55A	0223–2205	90.2	0.0400	0.0612	0.0212	53.0 ^b
U56A	0223–2205	75.8	0.1400	0.1202	–0.0198	14.1
U57A	0223–2205	106.5	0.2400	0.1969	–0.0431	18.0
U58A	1742–0000^c	81.1	0.3600	0.2929	–0.0671	18.6
U59A	1742–0000^c	98.8	0.4000	0.3238	–0.0762	19.1
V54A	<i>1554–2300</i>	<i>102.2</i>	<i>0.3800</i>	0.5333	0.1533	40.3
V55A	<i>1554–2101</i>	<i>141.0</i>	<i>0.3800</i>	0.2446	–0.1354	35.6
V56A	1742–2201	182.2	0.5100	0.2987	–0.2113	41.4
V57A	1742–2300	118.9	0.4700	0.1351	–0.3349	71.3
V58A	1742–0100^c	58.3	0.2000	0.1811	–0.0189	9.5
V59A	1742–0100^c	25.2	0.1800	0.1704	–0.0096	5.3
W54A	<i>1554–2300</i>	<i>22.7</i>	<i>0.0000</i>	0.0002	Trace	—
KMSC	<i>1554–0002^c</i>	<i>85.9</i>	<i>0.0400</i>	0.0214	–0.0186	46.5 ^c
W56A	<i>1554–0102^c</i>	<i>152.0</i>	<i>1.2600</i>	0.5541	–0.7059	56.0
W57A	1742–0200^c	147.9	0.4400	0.2937	–0.1463	33.3
W58A	1742–0200^c	98.4	0.9800	0.3308	–0.6492	66.2
W59A	1742–0301^c	55.4	0.2000	0.3586	0.1586	79.3
W60A	1742–0503^c	98.0	1.0400	0.2756	–0.7644	73.5

^a Doppler stations used for these observations are identified by their font type: regular font for KFCX (except stations T58A and T59A, which are covered by KAKQ), boldface for KRAX, and italics for KGSP.

^b Measurement results from rainfall observation that is possibly too low to be useful for the purpose of this statistical assessment.

^c End time (UTC) is actually on 14 Jun 2013.

the total rainfall measurements plotted for each TA station, while Fig. 8b displays the distance of each of these TA stations from their nearest Doppler stations versus the percentage offset of the DSP observations from the Vaisala observations. There is a trend of higher-percentage offsets among most of the stations

with greater distances, except for T54A, which reports a low-percentage difference from the DSP values with great distance, and W59A, which is the opposite. Also, U56A, U57A, U58A, and U59A appear to report lower-percentage differences in rainfall totals with greater distances. Since the Doppler scans conically

from each station, it is possible that the DSP product is not accurately measuring the total rainfall with greater distance (Mazari et al. 2013).

DATA ACQUISITION METHODS AND FUTURE DEPLOYMENTS. Over the lifespan of the USArray project its archive has reached a total data completeness of 98%. There are a couple of options for accessing the data from the TA network. As mentioned previously, all archived data are housed at the IRIS DMC and can be accessed via their web portal (www.iris.edu/ds/nodes/dmc/). Additionally, through collaboration with MesoWest at the University of Utah,

the 1-sps data from the TA's Setra 278 barometric pressure sensor are available to the public through a separate web-based portal (<http://meso1.chpc.utah.edu/usarray>). This site also combines historic and current Doppler data with other data products via MesoWest's numerous collaborations for those interested in quick data visualization. MesoWest has also published their work (Jacques et al. 2015).

As the pullout of the TA along the East Coast has progressed, a large number of stations have been transitioned into a somewhat less dense array called the Central Eastern United States Network (CEUSN; see Fig. 9a). The goal of the CEUSN array is to continue

in the spirit of the original TA network except the stations will remain in place for up to five years rather than rotate deployment. This was originally designed to accommodate the seismic monitoring capability of the TA network; however, the surface pressure monitoring capabilities will still exist at those stations. By the end of the CEUSN deployment, many of these stations will have 1- and 40-sps surface pressure data for up to approximately seven years.

Perhaps the most exciting opportunity for meteorological observations and applications from the TA network lay just on the horizon. The TA network is currently being installed throughout Alaska and will reach about 300 stations with a grid spacing of approximately 85 km by 2018. There are large regions in Alaska that do not have meteorological equipment deployed (Fig. 9b), and therefore the TA's plan to have 1-sps surface barometric readings in such isolated locations will present new data opportunities for the meteorological community. We anticipate up to 100 of these locations will include the Vaisala WXT520 weather station.

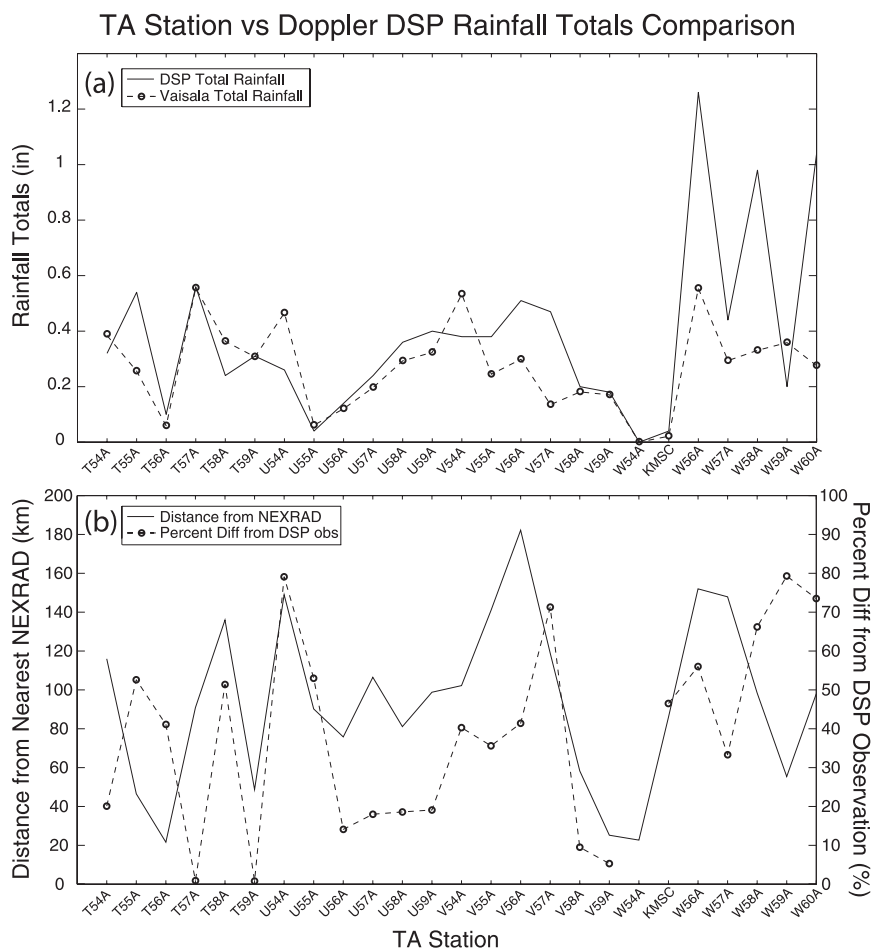


FIG. 8. (a) Total rainfall observed by the DSP product (solid line) and Vaisala (dashed line, circles) per TA station along the x axis. (b) Percentage offset of the Vaisala data from the NEXRAD level III DSP product (right y axis; dashed line, circles) vs the distance of that TA station from its nearest WSR-88D station (left Y axis; solid line). The percentage value has been dropped at W54A, where there were trace observations. There appears to be a trend in the data that suggests a greater-than-30% offset between the DSP and Vaisala observations where the distances were higher (i.e., U54A, V56A, V57A, W56A, and W57A), though not always (i.e., T54A and W59A). Please note that, for T56A, U55A, and KM5C, it is possible that the rainfall measurements were too low to get an accurate comparison.

Unlike the standard TA vault installation depicted in Fig. 2, station installations in Alaska will conform to a different installation strategy. Seismometers will instead be placed within boreholes while the rest of the equipment will be housed within specially protected huts (see www.usarray.org/alaska for further details). To negotiate the challenges of transmitting data from these Alaska deployments, the stations are being configured to provide data in burst packets over satellite connections. Furthermore, to reduce data packet size, the Hyperion infrasound and Setra 278 pressure data will only be transmitting their 1-sps data channels. We expect that during the colder months most of stations with exterior Vaisala units will be unable to report wind speeds and directions, and perhaps more observations, because of riming and snowfall accumulation, but they should still be available to provide data during the warmer months. Surface pressure monitoring should remain uninterrupted and accessible through the burst satellite communication.

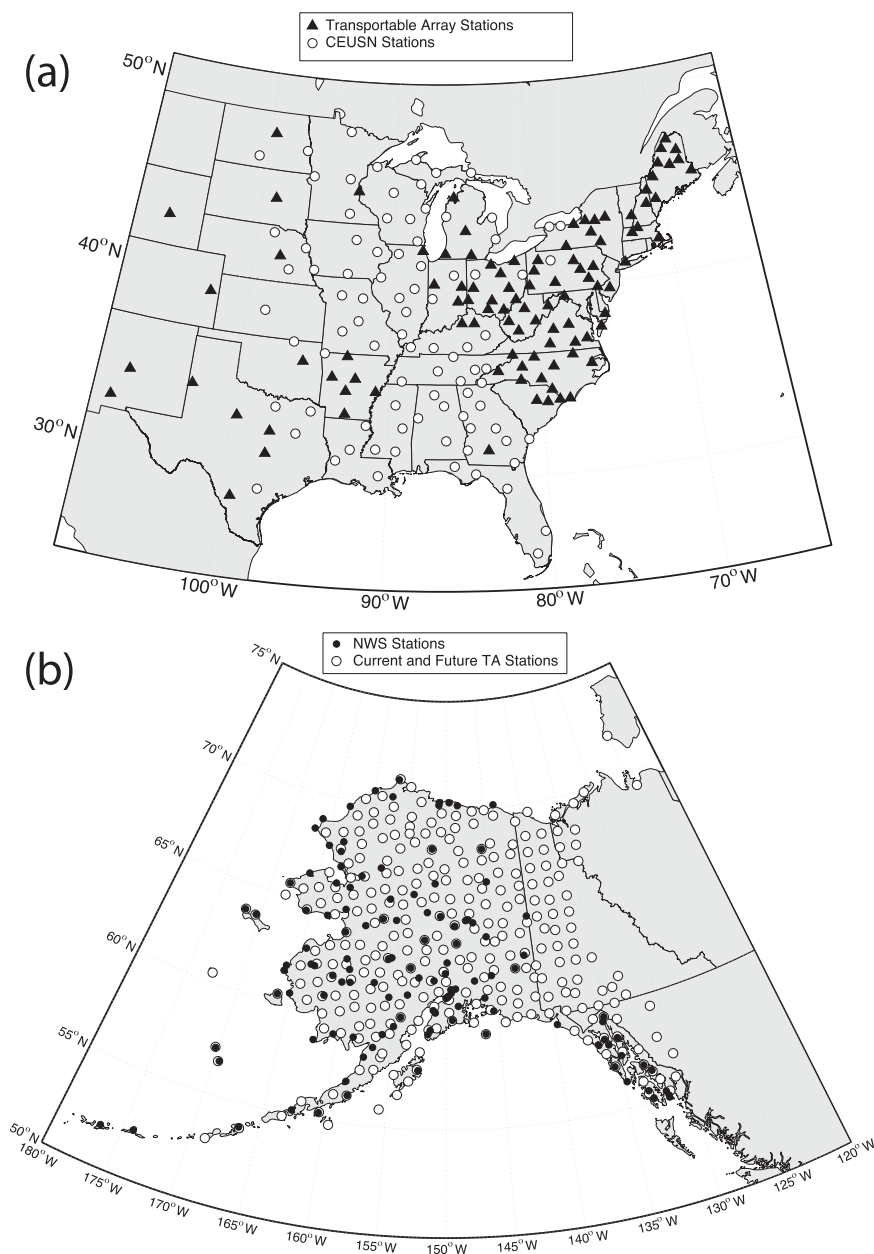


FIG. 9. (a) Map of the TA stations to be incorporated in the CEUSN network (black triangles) and current CEUSN stations (white circles) as of the end of Nov 2014. (b) Map of current and future TA station installations in AK and YT in Canada (white dots) plotted with the NWS stations (black dots) as of 5 Aug 2014. Large regions of AK, including much of the northern area of the state, will be monitoring surface barometric pressure where the NWS does not have equipment in place.

DISCUSSION. The Cartesian design, high-frequency sampling, and real-time acquisition capabilities of the USArray Transportable Array's (TA) network make it an unexpected but nevertheless useful platform for observational meteorology. This applies not only to localized severe weather events, but also to mesoscale and synoptic-scale weather phenomena.

The TA network has already been shown to be a suitable platform for infrasonic source location with previous work regarding gravity wave detection and propagation. Further potential in utilizing the TA data for high-frequency meteorological applications related to severe weather is also achievable. It may also be possible to isolate common pressure and seismic

signatures related to severe weather phenomena in order to help facilitate the construction of a real-time detection algorithm. This can bolster nowcast decision-making capabilities.

The potential does not end with just real-time applications, however, as several meteorological data products can be developed utilizing historical data from the TA network. Catalogs of weather observations can automatically be compiled and referenced. Pressure data can be utilized to validate forecast models. The addition of the Vaisala WXT520 allows for the monitoring of rain rates and further allows for the possibility for tuning precipitation models.

It may seem at first that the short-term design of the TA network and its grid spacing pose a limitation as a platform for observational meteorology. In fact, this paper demonstrates that the TA network represents a viable installation strategy for future multidisciplinary projects and initiatives that monitor and collect meteorological data.

ACKNOWLEDGMENTS. This material is based on work supported by the Incorporated Research Institutions for Seismology under their Cooperative Agreements EAR-1261681 and EAR-1358520 with the National Science Foundation, and by National Science Foundation Award AGS-0960275. Canadian map data are provided by the Natural Resources Canada, Nunavut Planning Commission. We thank the USArray station servicing crews for their diligent and very hard work throughout the entire USArray deployment. We would also like to thank Dr. Luciana Astiz for helping to motivate this publication forward.

REFERENCES

- Ansari, S., 2014: NOAA Weather and Climate Toolkit. NOAA/National Climatic Data Center. [Available online at www.ncdc.noaa.gov/wct/.]
- Arrowsmith, S. J., J. B. Johnson, D. P. Drob, and M. A. H. Hedlin, 2010: The seismoacoustic wavefield: A new paradigm in studying geophysical phenomena. *Rev. Geophys.*, **48**, RG4003, doi:10.1029/2010RG000335.
- Atkins, N. A., C. S. Bouchard, R. W. Przybylinski, R. J. Trapp, and G. Schmocker, 2005: Damaging surface wind mechanisms within the 10 June 2003 Saint Louis bow echo during BAMEX. *Mon. Wea. Rev.*, **133**, 2275–2296, doi:10.1175/MWR2973.1.
- Bedard, A. J., Jr., and M. J. Sanders, 1978: Thunderstorm-related wind shear detected at Dulles International Airport using a Doppler acoustic/microwave radar, a monostatic sounder and arrays of surface sensors. *Proc. Conf. on Weather Forecasting and Analysis and Aviation Meteorology*, Silver Spring, MD, Amer. Meteor. Soc., 347–352.
- , W. H. Hooke, and D. W. Beran, 1977: The Dulles airport pressure jump detector array for gust front detection. *Bull. Amer. Meteor. Soc.*, **58**, 920–926, doi:10.1175/1520-0477(1977)058<0920:TDAPJD>2.0.CO;2.
- De Angelis, S., and P. Bodin, 2012: Watching the wind: Seismic data contamination at long periods due to atmospheric pressure-field-induced tilting. *Bull. Seismol. Soc. Amer.*, **102**, 1255–1265, doi:10.1785/0120110186.
- de Groot-Hedlin, C. D., M. A. H. Hedlin, K. T. Walker, D. P. Drob, and M. A. Zumberge, 2008: Evaluation of infrasound signals from the shuttle Atlantis using a large seismic network. *J. Acoust. Soc. Amer.*, **124**, 1442–1451, doi:10.1121/1.2956475.
- , —, and K. T. Walker, 2013: Detection of gravity waves across the USArray: A case study. *Earth Planet. Sci. Lett.*, **402**, 346–352, doi:10.1016/j.epsl.2013.06.042.
- Doswell, C. A., III, G. W. Carbin, and H. E. Brooks, 2012: The tornadoes of spring 2011 in the USA: An historical perspective. *Weather*, **67**, 88–94, doi:10.1002/wea.1902.
- Fujita, T. T., and H. R. Byers, 1977: Spearhead echo and downburst in the crash of an airliner. *Mon. Wea. Rev.*, **105**, 129–146, doi:10.1175/1520-0493(1977)105<0129:SEADIT>2.0.CO;2.
- Fulton, R. A., J. P. Breidenbach, D. Seo, and D. A. Miller, 1998: The WSR-88D rainfall algorithm. *Wea. Forecasting*, **13**, 377–395, doi:10.1175/1520-0434(1998)013<0377:TWRA>2.0.CO;2.
- Hedlin, M. A. H., D. Drob, K. Walker, and C. D. de Groot-Hedlin, 2010: A study of acoustic propagation from a large bolide in the atmosphere with a dense seismic network. *J. Geophys. Res.*, **115**, B11312, doi:10.1029/2010JB007669.
- , C. D. de Groot-Hedlin, and D. P. Drob, 2012a: A study of infrasound propagation using dense seismic network recordings of surface explosions. *Bull. Seismol. Soc. Amer.*, **102**, 1927–1937, doi:10.1785/0120110300.
- , K. Walker, D. P. Drob, and C. D. de Groot-Hedlin, 2012b: Infrasound: Connecting the solid Earth, oceans and atmosphere. *Annu. Rev. Earth Planet. Sci.*, **40**, 327–354, doi:10.1146/annurev-earth-042711-105508.
- Houze, R. A., Jr., 1993: *Cloud Dynamics*. Academic Press, 573 pp.
- Istok, M. J., and Coauthors, 2009: WSR-88D dual polarization initial operational capabilities. Preprints, *25th Conf. on Interactive Information and Processing*

- Systems (IIPS) for Meteorology, Oceanography, and Hydrology*, Phoenix, AZ, Amer. Meteor. Soc., 15.5. [Available online at <https://ams.confex.com/ams/pdffpapers/148927.pdf>.]
- Jacques, A. A., J. D. Horel, E. T. Crosman, and F. L. Vernon, 2015: Central and eastern U.S. surface pressure variations derived from the USArray network. *Mon. Wea. Rev.*, **143**, 1472–1493, doi:10.1175/MWR-D-14-00274.1.
- Kanamori, H., J. Mori, D. L. Anderson, and T. H. Heaton, 1991: Seismic excitation by the space shuttle Columbia. *Nature*, **349**, 781–782, doi:10.1038/349781a0.
- Klimowski, B. A., M. J. Bunkers, M. R. Hjelmfelt, and J. N. Covert, 2003: Severe convective windstorms over the northern high plains of the United States. *Wea. Forecasting*, **18**, 502–519, doi:10.1175/1520-0434(2003)18<502:SCWOTN>2.0.CO;2.
- Klinge, D. L., D. R. Smith, and M. M. Wolfson, 1987: Gust front characteristics as detected by Doppler radar. *Mon. Wea. Rev.*, **115**, 905–918, doi:10.1175/1520-0493(1987)115<0905:GFCADB>2.0.CO;2.
- Langston, C., 2004: Seismic ground motions from a bolide shock wave. *J. Geophys. Res.*, **109**, B12309, doi:10.1029/2004JB003167.
- Lee, J. J., T. M. Samaras, and C. R. Young, 2004: Pressure measurements at the ground in an F-4 tornado. Preprints, *22nd Conf. on Severe Local Storms*, Hyannis, MA, Amer. Meteor. Soc., 15.3. [Available online at <https://ams.confex.com/ams/pdffpapers/81700.pdf>.]
- Mazari, N., H. Xie, J. Zeitler, and H. O. Sharif, 2013: Validation of the NEXRAD DSP product with a dense rain gauge network. *J. Hydrol. Eng.*, **18**, 156–157, doi:10.1061/(ASCE)HE.1943-5584.0000676.
- Nishiyama, R. T., and A. J. Bedard Jr., 1991: A “Quad-Disc” static pressure probe for measurement in adverse atmospheres: With a comparative review of static pressure probe designs. *Rev. Sci. Instrum.*, **62**, 2193–2204, doi:10.1063/1.1142337.
- Pryor, S. C., R. Conrick, C. Miller, J. Tytell, and R. J. Barthelmie, 2014: Intense and extreme wind speeds observed by anemometer and seismic networks: An eastern U.S. case study. *J. Appl. Meteor. Climatol.*, **53**, 2417–2429, doi:10.1175/JAMC-D-14-0091.1.
- Sorrells, G. G., J. A. McDonald, Z. A. Der, and E. Herrin, 1971: Earth motion caused by local atmospheric pressure changes. *Geophys. J. Roy. Astron. Soc.*, **26**, 83–98, doi:10.1111/j.1365-246X.1971.tb03384.x.
- Sufri, O., K. D. Koper, R. Burlacu, and B. de Foy, 2013: Microseisms from Superstorm Sandy. *Earth Planet. Sci. Lett.*, **402**, 324–336, doi:10.1016/j.epsl.2013.10.015.
- Tatom, F. B., 1993: Seismic detection of tornadoes. *Earthquakes Volcanoes*, **24**, 222–234.
- , and S. J. Vitton, 2001: The transfer of energy from a tornado into the ground. *Seismol. Res. Lett.*, **72**, 12–21, doi:10.1785/gssrl.72.1.12.
- , K. R. Knupp, and S. J. Vitton, 1995: Tornado detection based on seismic signal. *J. Appl. Meteor.*, **34**, 572–582, doi:10.1175/1520-0450(1995)034<0572:TD BOSS>2.0.CO;2.
- Tytell, J. E., F. Vernon, and J. Eakins, 2011: Tracking outflows from severe thunderstorms using NSF Earth Scope USArray pressure sensors. *Proc. 24th Conf. on Weather and Forecasting/20th Conf. on Numerical Weather Prediction*, Seattle, WA, Amer. Meteor. Soc., 2A.3. [Available online at <https://ams.confex.com/ams/91Annual/webprogram/Paper180739.html>.]
- Vernon, F. L., J. Eakins, J. E. Tytell, B. Busby, and B. Woodward, 2011: Observations of weather phenomena by NSF Earth Scope USArray seismic and pressure sensors. *Proc. 24th Conf. on Weather and Forecasting/20th Conf. on Numerical Weather Prediction*, Seattle, WA, Amer. Meteor. Soc., 110. [Available online at <https://ams.confex.com/ams/91Annual/webprogram/Paper180671.html>.]
- Walker, K. T., M. A. H. Hedlin, C. D. de Groot-Hedlin, J. Vergoz, A. Le Pichon, and D. Drob, 2010: Source location of the 19 February 2008 Oregon bolide using seismic networks and infrasound arrays. *J. Geophys. Res.*, **115**, B12329, doi:10.1029/2010JB007863.
- , R. Shelby, M. A. H. Hedlin, C. D. de Groot-Hedlin, and F. L. Vernon, 2011: Western U.S. Infrasonic Catalog: Illuminating infrasonic hotspots with the USArray. *J. Geophys. Res.*, **116**, B12305, doi:10.1029/2011JB008579.
- Wallace, J. M., and P. V. Hobbs, 1977: *Atmospheric Science: An Introductory Survey*. Academic Press, 350 pp.
- Zürn, W., and R. Widmer, 1995: On noise reduction in vertical seismic records below 2 mHz using local barometric pressure. *Geophys. Res. Lett.*, **22**, 3537–3540, doi:10.1029/95GL03369.

AMS titles now available as eBooks at **springer.com**

AMS BOOKS

RESEARCH APPLICATIONS HISTORY

www.ametsoc.org/amsbookstore



Scan to see
AMS eBook titles
at springer.com



AMERICAN METEOROLOGICAL SOCIETY